Preparation and Properties of Polyimide Nanocomposites via a Soluble Polyisoimide Precursor

Seung Bae Oh, Young Jun Kim, Ji Heung Kim

Department of Chemical Engineering, Polymer Technology Institute, Sungkyunkwan University, 300 Chunchun, Jangan, Suwon, Kyonggi 440-746, Korea

Received 4 December 2004; accepted 6 June 2005
DOI 10.1002/app.22753
Published online in Wiley InterScience (www.interscience.wiley.com).

ABSTRACT: A polyisoimide based on 4,4′-oxydiphthalic dianhydride and 4,4′-oxydianiline was synthesized and used for the preparation of nanocomposites with commercial organoclays by the solution dispersion technique. The cast composite films were heat-treated to convert them into polyimide nanohybrid films. Homogeneous dispersions were obtained at lower clay concentrations (<5 wt %), and this was confirmed by X-ray diffraction and transmission electron microscopy. The nanocomposites displayed improved thermal and mechanical properties. © 2005 Wiley Periodicals, Inc. J Appl Polym Sci 99: 869–874, 2006

Key words: organoclay; nanocomposites; polyimides; high-performance polymers

INTRODUCTION

Polyimides (PIs) have found many applications as high-temperature insulators and dielectrics, adhesives, and matrices for high-performance composites because of their excellent electrical, thermal, and high-temperature mechanical properties. Efforts have been directed toward the synthesis and characterization of polyisoimides (PIIs) to develop novel soluble precursors of PIs. The fact that PIIs possess improved solubility and can be converted to PIs without the formation of water (or other volatile byproducts) could be advantageously used in the fabrication of void-free laminates and adhesive joints.[1] Also, polymer/inorganic nanocomposites have recently received considerable attention because they often exhibit superior physical, mechanical, and thermal properties in comparison with conventional composites or unfilled polymers. Lately, there have been a considerable number of publications associated with the preparation and properties of PI–clay nanocomposites.[2–9] Usually, rigid and aromatic PIs are insoluble and show limited processability, and so soluble poly(amic acid) precursors are frequently used for solution dispersion, or sometimes an in situ polymerization method is employed. In this work, an organosoluble PII, typically from 4,4′-oxydiphthalic dianhydride (ODPA)/4,4′-oxydianiline (ODA), was synthesized and used for the preparation of nanocomposites with commercial organoclays [or organically modified montmorillonites (OMMTs)]. By a thermal curing process, the PII–clay was converted into PI–clay nanocomposite films. The intercalation behavior and thermal and mechanical properties of the composites in cast films were investigated.

Correspondence to: J. H. Kim (kimjh@skku.edu).

Journal of Applied Polymer Science, Vol. 99, 869–874 (2006)

EXPERIMENTAL

Materials

Two different organoclays, that is, Cloisite 10A (C10A) and Cloisite 30B (C30B), were supplied by Southern Clay Products and used after sieving through a 325-mesh sieve. C10A has a cation-exchange capacity of 125 mequiv/100 g, and C30B has a cation-exchange capacity of 90 mequiv/100 g. ODPA and ODA were obtained from Sigma–Aldrich Co. and were purified by sublimation in vacuo. 1,3-Dicyclohexyl carbodiimide (DCC) and 1-methyl-2-pyrrolidinone (NMP; anhydrous) were purchased from Sigma–Aldrich and used as received. Other common reagents were used without purification.

Preparation of PII

PII was synthesized from ODA and ODPA in NMP at room temperature (see Scheme 1).[1] ODA (4.0518 g, 20.235 mmol), ODPA (6.2044 g, 20 mmol), and NMP (10 mL) were placed in a 250-mL, four-necked, round-bottom flask equipped with a mechanical stirrer and a nitrogen inlet and outlet. This mixture was stirred at room temperature for 24 h under nitrogen, and phthalic anhydride (0.083 g, 0.56 mmol) was added. To the prepared poly(amic acid) solution, DCC (9.0785 g, 44 mmol) was added, and the reaction mixture was

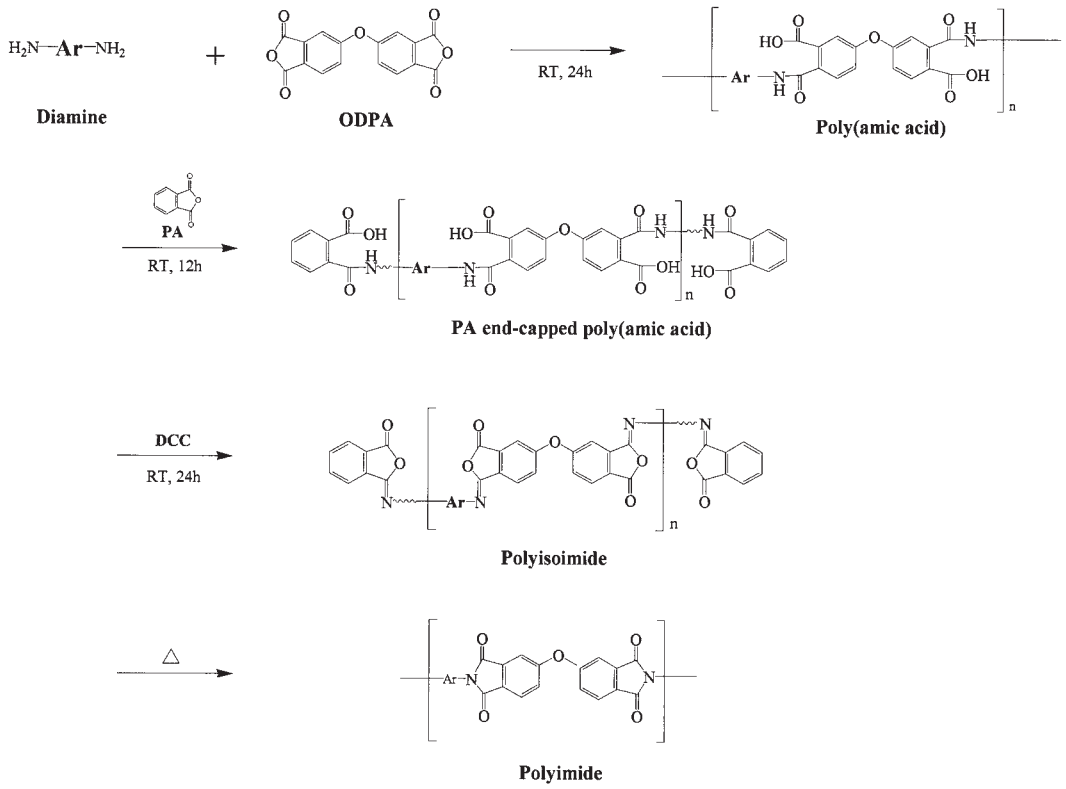

Scheme 1 Schematic diagram of the synthesis of PII.

stirred for an additional 24 h at room temperature. The formed solid, dicyclohexyl urea, was filtered off, and the collected PII solution was poured into a large excess amount of isopropyl alcohol. The precipitated PII was filtered off and dried in vacuo at 80°C for 72 h.

Preparation of the PI/organoclay nanocomposite films

An organoclay (OMMT) at a concentration of 1, 3, 5, or 7 wt % with respect to PII was dispersed in NMP under magnetic stirring for 24 h at room temperature. Solutions (4 w/v %) in NMP for PII composites were prepared by the addition of PII to each of the dispersed organoclay solutions. After the treatment of the solutions with an ultrasonic processor for 10 min, the resulting solutions were cast onto 12 × 7 cm^2 glass slides and dried in vacuo at 50°C for 24 h, and then the cast films were thermally cured at 100 and 200°C for 1 h each and then at 280°C for 30 min (Fig. 1).

Measurements

IR spectra were recorded with a PerkinElmer Spectrum 2000. Wide-angle X-ray diffraction (XRD) patterns were recorded on a Rigaku Rotaflex D/MAX diffractometer with Cu Kα radiation (40 kV, 50 Ma). XRD experiments were performed in the range of 2θ = 3–30° at a scanning rate of 3°/min. The thermal properties were examined under an N_2 atmosphere with a PerkinElmer TGA/DSC 7 instrument at a heating rate of 10°C/min. The modulus and glass-transition temperature were measured on a dynamic me-

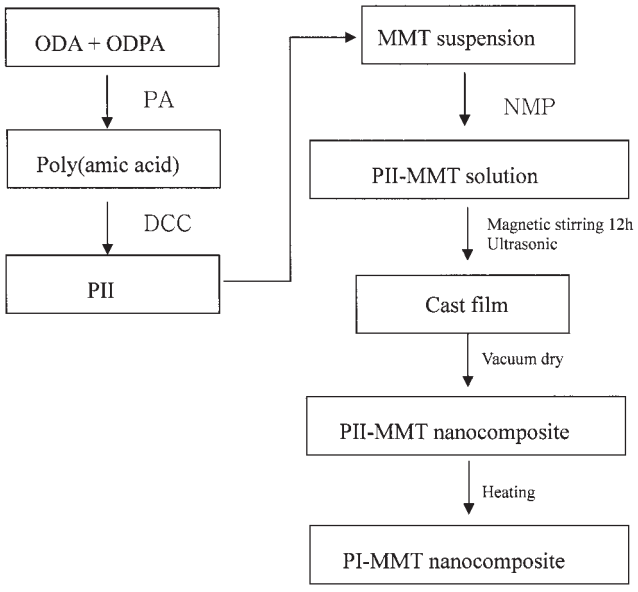

Figure 1 Flow chart of PI/organoclay nanocomposite preparation.

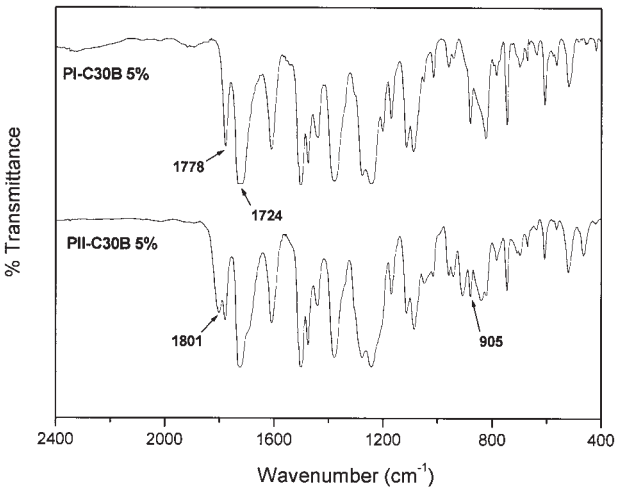

Figure 2 FTIR spectra of PII and cured PI.

chanical analyzer (Seiko Exstar 6000, Seico Instruments, Japan) at a heating rate of 5°C/min and at a frequency of 1 Hz. The tensile properties of the films were measured on an LR 30K materials testing machine (Lloyd Instrument, Ltd.) at a crosshead speed of 2 mm/min. Transmission electron microscopy (TEM) photographs of ultrathin sections of PI/organoclay samples were taken on a JEM 1010 (JEOL, Japan) transmission electron microscope with an acceleration voltage of 80 kV. The samples were prepared by the placement of the ODA–ODPA/organoclay films in epoxy capsules and then by the curing of the epoxy at 70°C for 24 h in a vacuum oven. Subsequently, the cured epoxies containing the ODA–ODPA/organoclay were microtomed with a Leica Ultracut Uct into 90-nm-thick slices in a direction normal to the plane of the film. A layer of carbon about 1 nm thick was deposited on these slices, which were on 200-mesh copper nets for TEM observation.

RESULTS

PII with an inherent viscosity of 0.83 dL/g (NMP) was successfully synthesized, and the structure was confirmed by FTIR spectroscopy. The IR spectrum of PII shows characteristic bands at 1800 and 905 cm^{-1}, which correspond to the carbonyl stretching and the isoimide ring vibration, respectively. The conversion to PI was confirmed by the observation of characteristic absorption bands of carbonyl stretching of imide groups (1778 and 1724 cm^{-1}; Fig. 2). The prepared PII was soluble in NMP and showed slight solubility in dimethylacetamide, dimethylformamide, and dimethyl sulfoxide. The differential scanning calorimetry (DSC) curves of PII show an exothermal peak in the first scan, which corresponds to the thermal imidization (283–385°C), and the glass transition from the second scan corresponding to PI was observed at 262°C (Fig. 3).

PI–organoclay composite films were prepared from two different commercial organoclays (C10A and C30B) showing similar behavior. A homogeneous (partially exfoliated) dispersion at a lower clay concentration (<5 wt %) was obtained, as determined by the optical clarity of the cast films and XRD patterns (Fig. 4). In the XRD patterns of PII composites with 1 and 3 wt % C10A or C30B, as shown in Figure 4(a,b), no obvious clay peaks can be observed in the curves. At a higher clay concentration of 5 or 7 wt %, however, XRD showed a peak indicating partial aggregation present along with the intercalated silicate layers presumably.

Figure 5 shows XRD patterns of two PI/organoclay composites obtained after thermal curing process under nitrogen in the range of 2θ = 12–25° for various clay loadings. The pure PI films display a broad peak at 2θ = 12–25°, and this peak can also be found in the PI/organoclay composites. For the PI composites with 1 wt % C10A or C30B, as shown in Figure 5, no obvious clay peaks can be observed in the XRD curves. This indicates that the silicate layers of the clay were exfoliated and dispersed homogeneously and randomly throughout the nanocomposite films. In the case of a 3 wt % concentration, peaks with low intensity are noticeable at about 6.7°, in contrast to PII composites with the same composition showing no peaks. This can probably be attributed to partial reaggregation that may have occurred during the thermal treatment and accompanying structural reorganization toward PI. When the concentration of the organoclay in PI exceeded 3 wt %, peaks at 2θ = 5–7° were observed, just as for the previous PII composites, in the XRD curves. This suggests that at higher clay loadings, some parts of the clay remain aggregated in

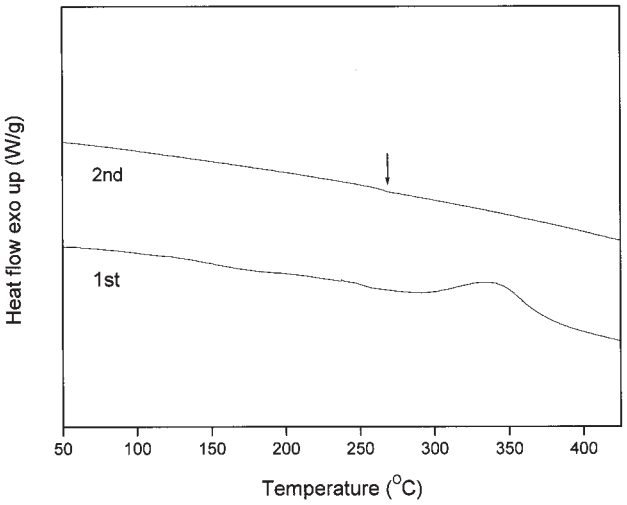

Figure 3 DSC thermograms of PII.

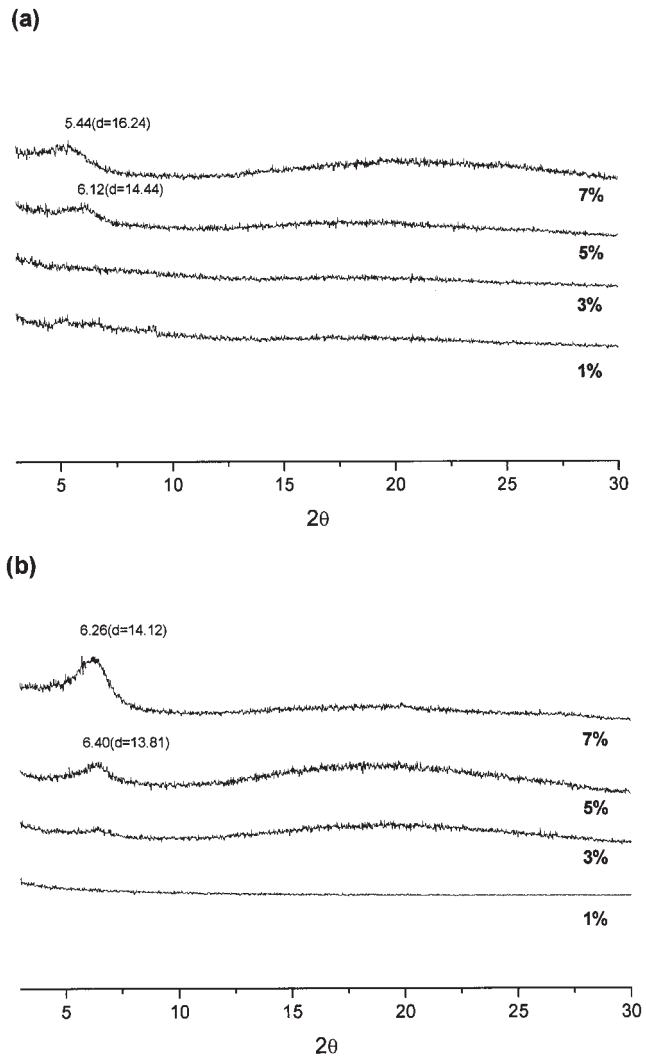

Figure 4 XRD patterns of (a) PII/C10A and (b)PII/C30B nanocomposites as a function of the organoclay loading.

the PI matrix. On the other hand, many researchers have reported that an organic intercalating agent in the interlayers of montmorillonite (MMT) might be detached from the surface of MMT during imidization.

The results obtained from the XRD patterns are complemented by the TEM micrographs shown in Figure 6. The black part represents the intersection of MMT layers, whereas the gray part represents the PI matrix. The TEM image of PI material incorporated with 3 wt % clay shows that the lamellar nanocomposite had a mixed nanomorphology. Individual silicate layers, along with two- and three-layer stacks, exfoliated in the PI matrix. Moreover, some larger intercalated tactoids could also be identified.

The dynamic mechanical properties of pure PI(ODA–ODPA) and PI/C10A composites at different temperatures are shown in Figure 7. In Figure 7(a), the storage modulus of the PI/C10A composites increased with the amount of organoclay in the temperature range of 50–300°C. Specifically, the largest increase in the storage modulus of these composites was for 93:7 PI/C10A (4.26 GPa), for which it was 320% larger than that of pure PI. The loss modulus of PI/C10A also increased with the amount of the organoclay, as shown in Figure 7(b). A broad maximum around 110°C and a sharp maximum at 253°C are displayed in the loss modulus curves of the PI/C10A composites. The low temperature at 110°C was caused by the rotation and oscillation of the phenyl group of ODA, and it was called the β relaxation, or subglass transition. The β relaxation of PI/C10A at different compositions took place at the same temperature, and this indicated that either the rotation or oscillation of the phenyl group of ODA was not affected by the presence of silicate layers. The high-temperature one, near 250°C, resulted from the backbone motion of the ODA–ODPA molecules, and it was called the α relaxation, or primary glass transition. The glass transition

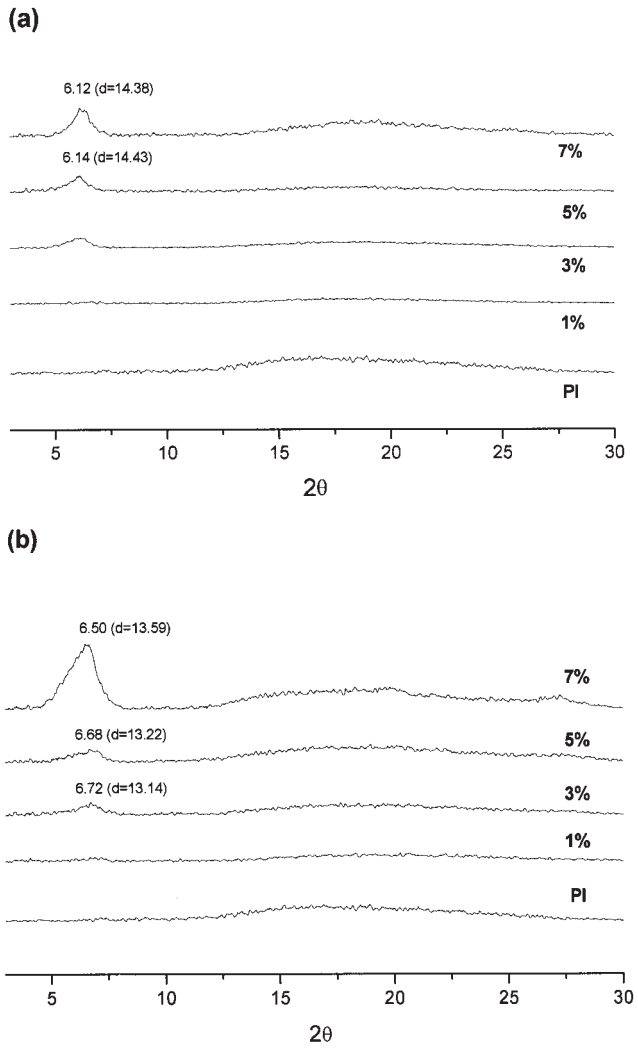

Figure 5 XRD patterns of (a) PI/C10A and (b)PI/C30B nanocomposites as a function of the organoclay loading.

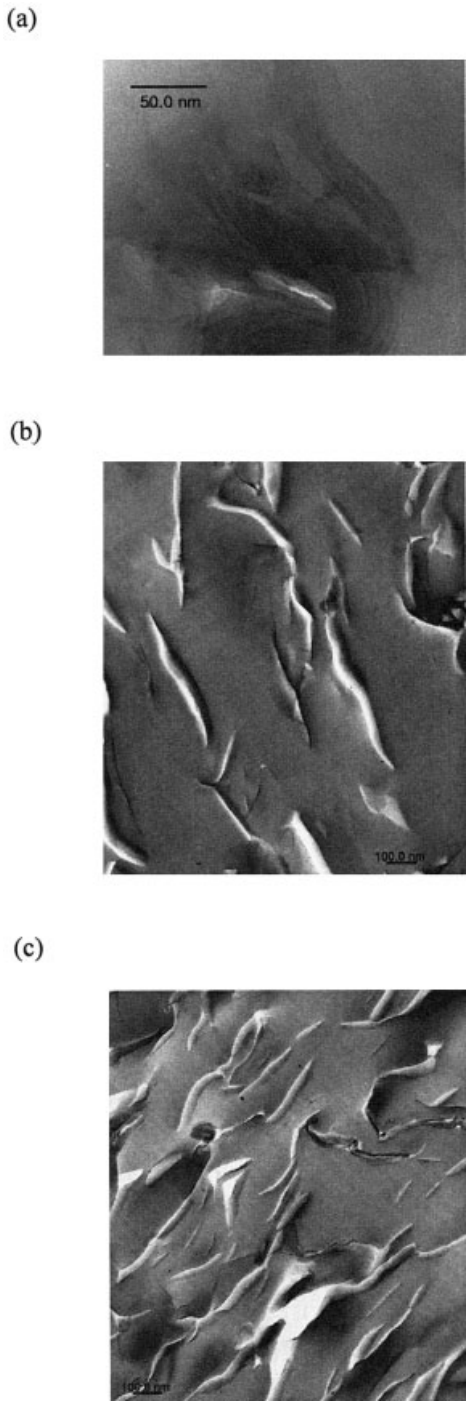

Figure 6 TEM micrographs of the cross-section view of (a) 97 : 3 PII/C10A, (b) 97 : 3 PI/C10A, and (c) 97 : 3 PI/C30B nanocomposite films.

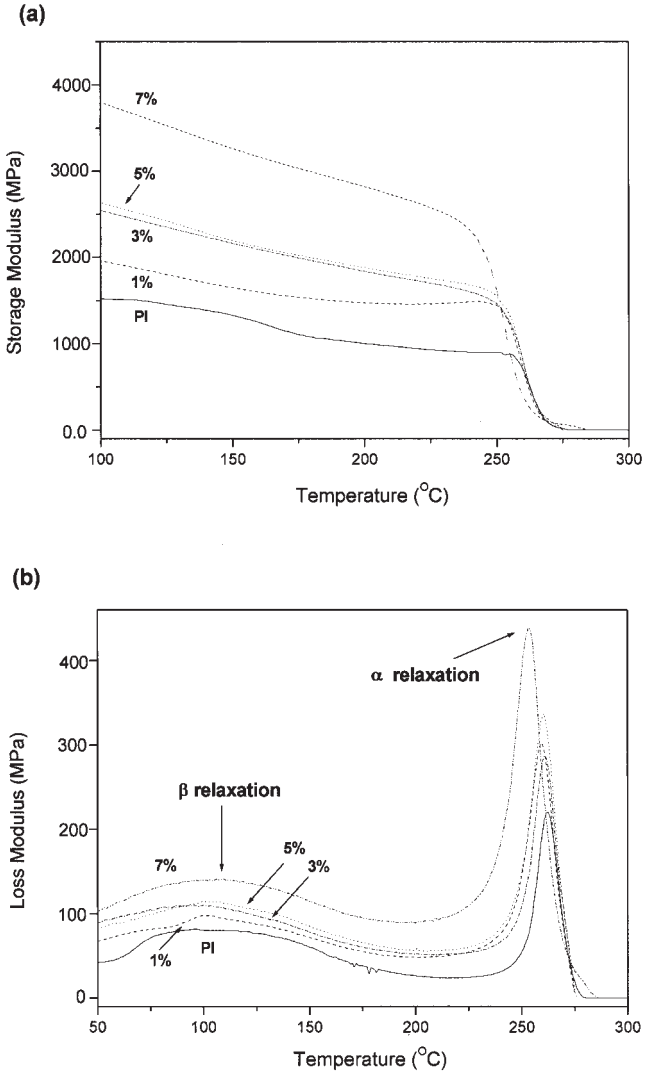

Figure 7 (a) Storage modulus and (b) loss modulus of PI/C10A nanocomposite films at different temperatures.

seems to decrease slightly with the amount of clay.[9] This suggests that the mobility of macromolecular chains becomes more flexible with the addition of organoclay, even though the reason is not clear yet.

The thermal and tensile properties of PI/C30B nanocomposite films are shown in Table I. The Young's modulus of the PI nanocomposites increased with the amount of the organoclay. For instance, a 68%

TABLE I
T_d and Mechanical Properties of PI/C10A and PI/C30B Nanocomposites

Clay type	Clay content (wt %)	T_d (°C)	Stress at the maximum load (MPa)	Young's modulus (GPa)	Strain at the maximum load (%)
C10A	0	585	61.2	1.45	10.8
	1	588	72.2	1.92	9.2
	3	595	78.6	2.43	7.4
	5	599	75.3	2.22	5.8
	7	581	74.2	2.06	4.1
C30B	0	585	61.2	1.45	10.8
	1	589	78.2	1.46	8.9
	3	595	74.3	1.57	7.2
	5	601	67.0	1.90	6.0
	7	607	58.6	2.00	3.8

increase in the modulus for the 97 : 3 PI/C10A composite film (2.43 GPa) was found, in comparison with that of pure PI (1.45 GPa). The maximum strength also increased up to around 128%, and the elongation decreased with the amount of clay; this means that the brittleness increased accordingly. A 38% increase in the modulus for the 93 : 7 PI/C30B composite film (2.00 GPa) was found, in comparison with that of pure PI (1.45 GPa). The decomposition temperatures (T_d's) of the nanocomposites tended to increase slightly as the clay content increased, and this indicated an improvement in the thermal stability of these nanocomposites.

CONCLUSIONS

Soluble PIIs from ODPA were synthesized, and their structure was confirmed by FTIR. The prepared PIIs showed excellent thermal stability and good solubility. PII/organoclay composite films were obtained by a solution method with two different organoclays and were thermally cured into PI/organoclay systems. The homogeneous dispersion was confirmed by XRD and TEM (<5 wt %). Organoclay/ODA–ODPA nanocomposites displayed increases in the modulus and in the maximum stress in comparison with pure ODA–ODPA. For instance, a 68% increase in the modulus for the 3 : 97 C10A/ODA–ODPA composite film (2.43 GPa) was found, in comparison with that of pure PI (1.45 GPa). The maximum strength also increased up to around 128%, but the elongation decreased with the amount of the clay. T_d's of the nanocomposites were higher than that of pristine PI.

References

1. Kim, Y. J.; Kim, J. S.; Choi, K.-Y. J Ind Eng Chem 2001, 7, 400.
2. Yeh, J. M.; Chen, C. L.; Kuo, T. H.; Su, W. F.; Huang, H. Y.; Liaw, D. J.; Lu, H. Y.; Liu, C. F.; Yu, Y. H. J Appl Polym Sci 2004, 92, 3573.
3. Cho, Y. H.; Park, J. M.; Park, Y. H. Macromol Res 2004, 12, 38.
4. Liang, Z. M.; Yin, J.; Xu, H. J. Polymer 2003, 44, 1391.
5. Delozier, D. M.; Orwoll, R. A.; Cahoon, J. F.; Ladislaw, J. S.; Smith, J. G., Jr.; Connell, J. W. Polymer 2003, 44, 2231.
6. Agag, T.; Koga, T.; Takeichi, T. Polymer 2001, 42, 3339.
7. Magaraphan, R.; Lilayuthalert, W.; Sirivat, A.; Schwank, J. W. Compos Sci Technol 2001, 61, 1253.
8. Nah, C.; Han, S. H.; Lee, J. H.; Lee, M. H.; Lim, S. D.; Rhee, J. M. Compos B 2004, 35, 125.
9. Tyan, H. L.; Wei, K. H.; Hsieh, T. E. J Polym Sci Part B: Polym Phys 2000, 38, 2873.